Global NEST Journal, Vol 27, No 2, 06485

Enhanced photocatalytic degradation of azo dyes using hydrothermally synthesized vanadium pentoxide nanomaterials

Natrayan Lakshmaiya[1]
[1]Department of Mechanical Engineering, Saveetha School of Engineering, SIMATS, Chennai, 602 105, Tamil Nadu, India
Received: 18/07/2024, Accepted: 29/10/2024, Available online: 14/12/2024
*to whom all correspondence should be addressed: e-mail: natrayanphd@gmail.com
https://doi.org/10.30955/gnj.06485

Graphical abstract

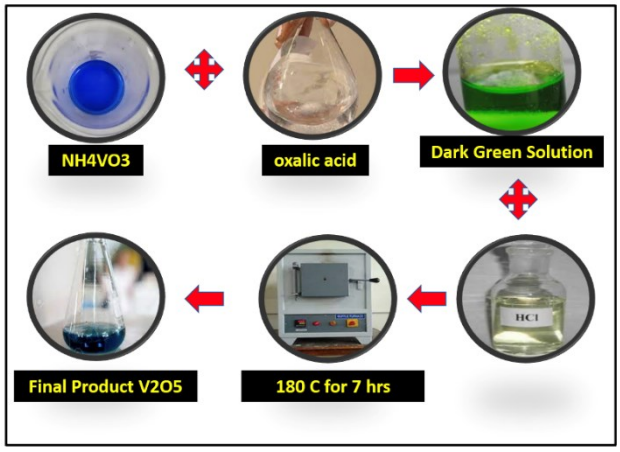

Abstract

This study employed a simple hydrothermal (HT) approach to synthesize vanadium pentoxide (V_2O_5) nanomaterials. The inherent limitations of V_2O_5, including low quantum efficiency and insufficient light sensitivity, restrict its potential for enhanced photocatalytic activity. The study investigates the photodegradation of methyl orange (MO) and Congo red (CR) dyes through annealing. X-ray diffraction (XRD) and Raman spectroscopy confirm the composition of V_2O_5, while SEM is used to observe the morphology of encapsulated nanoparticles. The bandgap of V_2O_5 is estimated to be between 2.51 and 2.73 eV using ultraviolet-visible (UV) spectroscopy. Additionally, the photodegradation of methylene blue (MB) dye is analyzed, with calcinated V2O5 achieving a 76% degradation efficiency of MB in 90 minutes. For CR and MO, degradation rates reached 97.91% and 86% within 200 minutes at a 20 mg/L dye concentration. The reaction rate constant for MB degradation was determined to be 8.19 x 10^{-5} s^{-1}. Overall, the HT-synthesized V_2O_5 exhibited enhanced photocatalytic activity due to its improved visible light absorbance, facilitating more effective photodegradation of azo dyes.

Keywords: Wastewater treatment; Methyl orange; Congo red; Vanadium pentoxide; Methylene blue; Hydrothermal method; Photocatalytic degradation; Nanomaterials.

1. Introduction

Transistor nanocomposite photocatalysts have received much interest recently because of their unique elemental composition compared to their bulk counterparts. They are currently at the vanguard of practical ecological and energy studies. A photocatalytic substance is a substance that is formed by absorbing a light ray and is capable of speeding up a chemical process without being destroyed [Sajid *et al.* 2020; Babar *et al.* 2022]. During the accelerated oxidised photocatalysts (AOP) method, the catalysts become activated by contact with light with photons greater than or equivalent to the photocatalyst's band gap energies (hv Eg). A primary stage of the procedure is creating a lone pair (EHP) upon dissociation. Such a picture helps electrons travel to the top of a silicon wafer and independently improve the reduction and oxidation of adsorption pieces. The lifespan of protons and voids impacts oxidation processes. For instance, structural flaws cause combinations to recombine and generate various trap locations, resulting in lower electron and hole concentrations. AOP is mainly used to purify coloured wastewater by trying to subvert organic substances. Researchers have paid close attention in recent decades to developing efficient graphene for treating wastewater [Habiba *et al.* 2019; Chen *et al.* 2018]. Many contaminants, such as natural chemicals, insecticides, and pharmaceuticals, are poisoning drinkable water due to rapid advancement in the agriculture and industry sectors. Daily, these dangerous and irreversible contaminants in the environment and groundwater increase. The issue with such contaminants is that they do not break down spontaneously and remain in nature for an extended period [George *et al.* 2022]. Colorants like methyl orange (MB), azo dyes (Rh-B), and Congo red are common sources of contaminants. MB is a major source of dye used in textile manufacturing; it is cancerous and damaging to both humans and the environment. All harmful contaminants must be degraded to lessen water contamination and transform them into freshwater resources. Given the significant advancements in the study, many technologies for degrading dyes and converting wastewater into acceptable water were developed, including photodegradation, microbiological approaches, and

transmembrane filtering [Lei *et al.* 2015]. The oxidising process is essential to deterioration. The advanced oxidation method involves photocatalysts, which reduce environmental pollution by decomposing colours into carbon dioxide and water. The photocatalyst decolourization method offers many benefits, including minimal cost, rapidity, and cold temperatures [Raja *et al.* 2023]. Photocatalysts with an adequate energy band gap, a vast interfacial ratio, reduced production, strong oxidative characteristics, and so on, are preferred for application in the decomposition processes. Scholars and researchers are interested in metal oxide compounds like titanium dioxide, CO_3O_4, V_2O_5, zinc, etc. Because of their prospective features include their large surface area, reduced heat dissipation, strong durability, and advantageous semiconductor composition [Sreeram *et al.* 2022].

Vanadium pentoxide (V_2O_5) is a metallic Vanadium oxyanion with a melting temperature of 956 K, a boiling temperature of 1920 K, and an energy band gap of 2.3 electron volts (eV). V_2O_5 does have a wide range of uses, including in potassium batteries, gas detection, oxidation accelerators, electrolytic capacitor values, and liquid crystal devices. The photocatalytic performance of V_2O_5 in dry powder creates a potential possibility for the breakdown of methanol, bromothymol blue, and solvents, among many other things. Its technique is based on the recombined energy per particle pair [Youssef *et al.* 2023; Camposeco *et al.* 2018]. This opening is large enough to oxidise a wide range of organic contaminants while producing oxygen radicals (OH) inside the drainage system [Yadav *et al.* 2023; Higashimoto *et al.* 2008]. The hole may oxidise an assortment of organic contaminants and also generate hydroxide ions (OH) in freshwater, while the electrons of a conduction and valence band interact with the oxide in H_2O to form oxidant radicals, which further interact with the OH -ion to form OH radicals. Because OH is a strong oxidizer, it destroys the contaminants by oxidising the organic compounds [Anwar *et al.* 2022]. Recent research has continued to explore the effectiveness of V_2O_5 nanomaterials in environmental applications. For instance, Bansal et al. (2023) demonstrated enhanced photocatalytic activity using functionalized V_2O_5 nano-adsorbents for water remediation [Bansal *et al.* 2023]. Youssef et al. (2023) reported successful degradation of methyl orange under solar irradiation using nano-vanadium oxides [Youssef *et al.* 2023]. Sreeram et al. (2022) investigated a novel indium vanadium oxide nanosheet-supported nickel-iron oxide nanoplate heterostructure, demonstrating enhanced photocatalytic degradation of tetracycline under visible light irradiation [Sreeram *et al.* 2022]. Babar et al. (2022) developed hydrothermally prepared vanadium oxide nanostructures and showcased their application in the photocatalytic degradation of organic dyes, highlighting improvements in surface area and stability [Babar *et al.* 2022]. Yadav et al. (2023) demonstrated the enhanced photocatalytic degradation activity of a V_2O_5/reduced graphene oxide (RGO) composite, showing significant improvements in the breakdown of methylene blue and other pollutants [Yadav *et al.* 2023]. Camposeco et al. (2018) studied incorporating vanadium oxide into various supports like TiO_2 and zeolite, resulting in improved photocatalytic efficiency under visible light, particularly for dye degradation [Camposeco *et al.* 2018]. These studies highlight the growing interest and efficacy of V_2O_5 in tackling water pollutants.

Present research considered the thermodynamic approach to effectively manufacture robust vanadium pentoxide in this study. The impact of heating on vanadium pentoxide photocatalysis efficiency for mono azo, diazo, and methylene blue dyes is investigated. The trigonal crystalline phase of V_2O_5 is shown by the extraordinarily strong X-ray diffraction (XRD) bands. The scanning electron microscope confirms the structure of flocculated nanoparticles (SEM). Spectroscopy reveals that absorption spectra occur mostly in the visual range, and V_2O_5 is a band gap material with an energy band gap value of 2.51-2.73 eV. The process of deterioration is also discussed in this paper.

2. Experimental Works

2.1. Material preparations

This study used A simple hydrothermal approach to effectively manufacture vanadium pentoxide nanomaterials. Vanadium pentoxide was prepared using analytical-grade ammonium metavanadate (NH_4VO_3), oxalic acid ($(COOH)_2H_2O$), and filtered water. First, 0.5 mol% of NH_4VO_3 precursors were mixed in 60 mL of quadruple-filtered water, which was constantly stirred with a stirring rod for 20 minutes to produce a white-coloured solution with a pH of 6. The resulting product was then carefully mixed with 0.7 M oxalate with constant mixing at 800 rpm until a deep green solution was formed.

The bacterial suspension was given 600 mL of deionized water. A few drops of HCl were added to preserve acidity in the range of 1-2, and then 120 mL of solvents were put into a 300 mL Titanium-Stainless (SS) sterilizer. The hydrothermal synthesis was carried out in a sealed stainless-steel autoclave at a temperature of 180°C for 7 hours. As a result, a dark blue sample solution and brown or black powders were formed as a finished product. The obtained sample was filtered, rinsed with demineralized water numerous times, and then evaporated at 120°C. Then, it was annealed at 400°C for 3 hours, yielding yellow. The entire process of synthesising vanadium pentoxide is depicted in Figure 1. The as-prepared and annealed V_2O_5 was designated as Specimens A and B for subsequent investigation.

2.2. Characterization analysis

To validate the produced V_2O_5, various characterization procedures are used. Its crystalline structure of V_2O_5 has been confirmed by employing CuK X-ray irradiation of wavelengths 1.53 on a Bruker D2 doppler device. The Bruker Multi-RAM equipment was used for the Raman analysis. Surface morphology was examined using JSM-IT200 scanning electron microscopy. Optics and photoluminescence were investigated using a System that automatically operated a UV-visible spectrometer. The catalytic efficiency of V_2O_5 against MB dye was investigated while a 320-watt filament lamp was positioned above the

reaction system. A luminosity meter was deployed to assess the brightness of visual light that reaches the MB solutions, which was also determined to be 97 Watts/m^2.

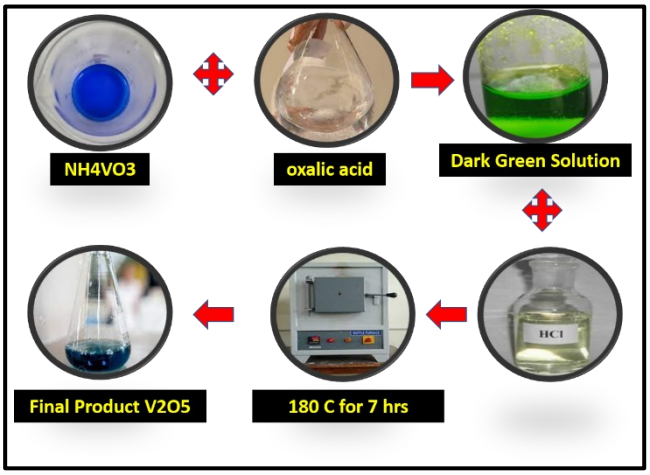

Figure 1. V_2O_5 synthesis process

2.3. Photocatalytic study

To test the photocatalytic performance of V_2O_5-NPs, liquid samples were subjected to a 320 W halogen lamp with a wavelength of 410 nm, which was employed as a visible illumination source to destroy MO and CR. The range between both the pipette and the lamps was 30 cm. For the kinetic research, dye mixtures at constant levels of 0.20 g/L (200 ml) were created; 100 mg of the as-made V_2O_5-NPs were combined in every reaction mixture individually. The pH of the solution remained about 5, and it was rapidly agitated for 20 minutes in the darkness before being exposed to visual light emission. Subsequently, the liquids were whirled at 8000 rpm for 4 minutes, and an evaporating dish was provided during the experiment to safeguard against thermal damage and to preserve the temperature at 0°C. The deterioration of a dye concentration was examined using a UV-Vis Perkins Beckman 30 spectroscope in the 200–700 nm wavelength spectrum.

The photocatalyst dye removal programme uses MB dyes like a modelling chemical. In this example, produced V_2O_5 was employed as a photocatalytic activity, while 15 ppm MB solutions were made and tested for deterioration. The pigment was maintained in the darkness and under the light for self-deterioration, and it immediately stopped but was available for degrading. During ultrasonic irradiation, a miniscule amount (10 mg) of V_2O_5 powders was disseminated in the dye concentration. As distributed V_2O_5 powder begins to degrade MB.

3. Result and discussions

3.1. Characterization analysis

3.1.1. XRD analysis

Substance characterization is carried out using the XRD method. The XRD patterns of specimens A and B are shown in Figure 2. The synthesised object's crystalline structure matches JCPDS Card No. 00-041-1431, which reveals the creation of an orthorhombic crystal lattice. The strong V_2O_5 spikes reflect material cleanliness and their crystalline nature. The spikes recorded at 16.25°, 19.63°, 22.34°, 27.19°, 32.56°, and 33.51° correspond to the lines (200), (001), (101), (110), (301), and (011). The sharp peak at 19.63° shows sufficient and consistent crystalline development along the c-axis (001) [Anwar *et al.* 2022].

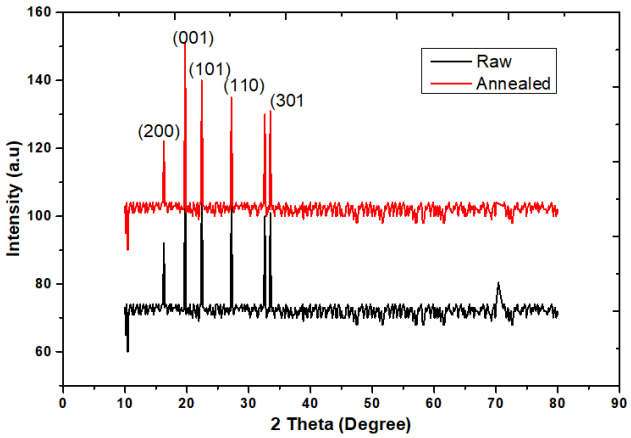

Figure 2. XRD Patterns of Prepared and Annealed NPs

The increasing amplitude and clarity of spikes (110), (310), (600), (020), and (710) following heating correlate to the object's improved crystallisation and frequency. The presence of residual peaks owing to the elimination of alkalis from these samples shows the impact after they were annealed at 600 °C. This Wacker equation is used to compute the crystalline phase. Using stochastic permit matching, the crystallinity size was determined to be 25 nm for specimen A and 56 nm for specimen B. The findings indicate that heating decreases the frequency range while increasing the crystalline nature [Bansal *et al.* 2023].

3.1.2. UV-visible spectroscopy

A UV-visible spectrophotometer is used to examine the optical properties of materials A and B. The absorbance spectrum and transmittance plot for energy band computation of specimens A and B, in which the impact of heating was detected, are shown in Figure 3. The spectra demonstrate that the absorption is mostly in the ultraviolet region, with heating causing a dramatic shift in the spectra. The heating action raises the lattice parameter (grain size) and reduces the object's band structure. The following formula calculates the substance's band structure [Youssef *et al.* 2023].

$$\left(ahv^2\right) = A\left(h_v - E_g\right) \quad (1)$$

A is the absorptivity, h is Planck's constant, v is photon wavelength, Eg is the object's band gap, and A is a fixed value. Because V_2O_5 has a straight band structure, n = 2. As illustrated in Figure 3, the absorption edge is computed from the junction of the divergent and, therefore is 2.51 and 2.73 eV for specimens A and B, respectively. The band gap values considered in this study are 2.51 eV for the prepared vanadium pentoxide (V_2O_5) and 2.73 eV for the annealed product, consistent with the reported values in the literature for V_2O_5. These results align with the research results of Kumar et al. (2011). The quantum size phenomenon causes the development and alteration of discrete energies in nanostructures, increasing the valence band of sensing materials. The conduction band of specimen A is larger because of the quantum collective oscillation.

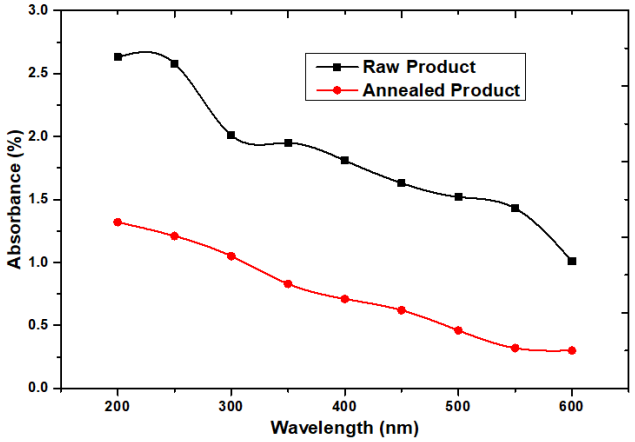

Figure 3. UV- Spectrum Analysis of prepared and annealed product

Compared to other commonly used photocatalytic materials, such as titanium dioxide (TiO_2) with a band gap of 3.2 eV and zinc oxide (ZnO) with a band gap of 3.37 eV, vanadium pentoxide has a relatively smaller band gap. This smaller band gap enables V_2O_5 to absorb more visible light, which enhances its photocatalytic efficiency under sunlight. However, materials such as cobalt oxide (CO_3O_4) with a band gap of around 2.1 eV perform similarly but may require different synthesis conditions. These comparisons suggest that V_2O_5 is competitive for applications requiring visible light absorption, making it suitable for photocatalytic degradation of organic dyes.

3.1.3. Microstructural Analysis

SEM is used to assess the surface appearance of sample A. SEM pictures of specimens A and B at various magnifications are shown in Figure 4. At increasing intensities, the microstructure of specimen A reveals the existence of nanomaterials. Such nanocrystals clump together and form a cluster. The SEM photos of specimens reveal the very same structure, but now with smaller nanocrystals. At the objects of study, such nanocrystals are evenly distributed and have varying shapes. The smaller size of V_2O_5 nanomaterials contributes to breakdown or may boost V_2O_5 degradation efficiency [Yang *et al.* 2010]. The SEM images reveal that the vanadium pentoxide nanoparticles exhibit a flocculated structure with uniform distribution. The morphology, characterized by small crystal sizes and large surface areas, is crucial in enhancing photocatalytic activity. A larger surface area increases the number of active sites for dye adsorption and subsequent degradation reactions. Additionally, the uniformity in the particle distribution helps maintain efficient charge transfer, thereby reducing the recombination of electron-hole pairs and improving photocatalytic efficiency. The clustered nanostructures observed in the SEM images also suggest that vanadium pentoxide can effectively disperse light, further contributing to its high photocatalytic activity under visible light.

3.1.4. Raman spectroscopy

The imprint for materials A and B in Raman is presented in Figure 5. The sharpness and cleanliness of the spikes indicate the effect of heating on the Raman spectra. Specimen A has spikes at 138.21, 271.52, 409.52, 521.36, and 691.63 cm-1. Compared to sample B, the amplitude and clarity of such summits are modest. The parallelism of a resource centre improves dramatically after tempering, as does the crystallisation of calcined V_2O_5. Spots at 141.36, 185.26, 273.11, 310.23, 410.15, 489.51, 521.40, 710.03, and 981.26 cm-1 suggest that the specimen has enhanced regularity and crystalline structure [Jasrotia *et al.* 2025].

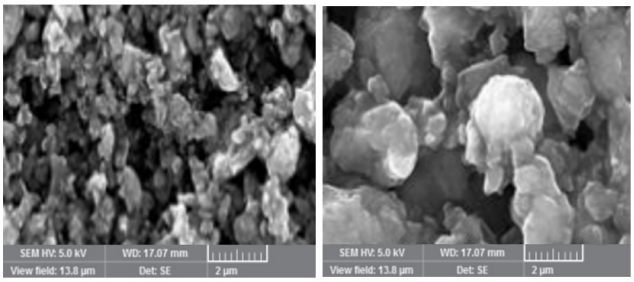

Figure 4. Microstructural Images of V_2O_5 Nanoparticles

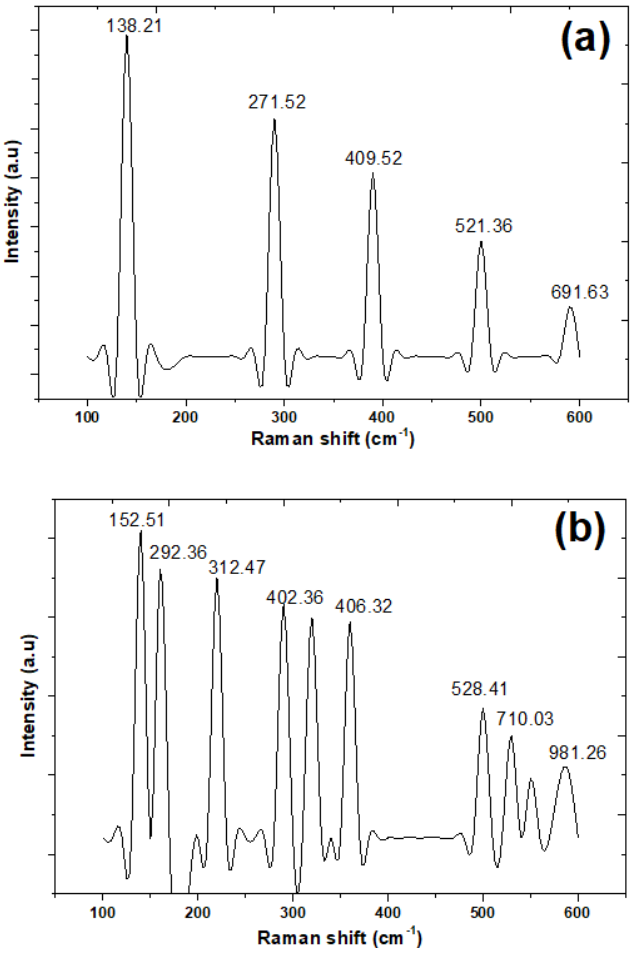

Figure 5. Raman Spectrum Analysis of (a) prepared; (b) Annealed product.

The 521.40 cm-1 spike has a typical crest, which correlates to V-O2 asymmetric stretching. Its spikes at 310.23, 410.15, and 981.26 cm1 are the object's performance levels, confirming the highly crystalline atomic structure. O-V-O has a bend modal frequency of 185.26 cm-1. Absorption bands at V=O and V2-O cause maxima at 710.03 and 981.26 cm-1, correspondingly.

The Raman peaks observed in the spectra provide important insights into the structural properties of the vanadium pentoxide nanomaterials. The sharp peak at 521.40 cm^{-1} corresponds to the V-O2 asymmetric

stretching, which is a key indicator of the crystalline quality of the V_2O_5 structure. Peaks at 710.03 cm^{-1} and 981.26 cm^{-1} are attributed to the V=O stretching and bending modes, respectively, which confirm the presence of strong V=O bonds in the vanadium pentoxide lattice. The lower frequency peaks around 138.21 cm^{-1} and 185.26 cm^{-1} correlate with O-V-O bending modes, reflecting the oxygen coordination environment in the material. These well-defined peaks suggest that the material has high crystallinity with minimal structural defects. The clarity and intensity of these peaks, particularly after annealing, indicate an improvement in the structural regularity and the enhanced formation of well-ordered V_2O_5 nanoparticles, which directly contribute to the material's improved photocatalytic efficiency.

3.2. Photocatalytic Activities

3.2.1. Photocatalytic Actions of Methyl Orange and Congo Red

The photocatalytic capacity of V_2O_5-NPs was measured using two different dye concentrations, Methyl Orange (MO) and Congo Red (CR), and a photosensitizer, a 300 W Halogen lamp at 410 nm. MO and CR are mono azo and diazo phenol derivative pigments recognised as hazardous substances and widely employed to colour leather shoes, fabrics, and various foods. The typical absorption band of MO is oriented up at 436 nm, whereas the absorbance value for CR decomposition is recorded at 453 nm. As shown in Figures 6 and 7, the sharp peaks faded over time, indicating dye concentration decolourization and pigment breakdown [Patil and Murthy 2016].

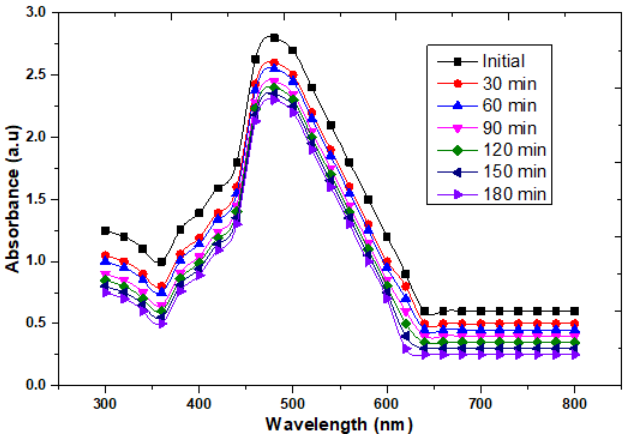

Figure 6. Absorption Spectrum of Methyl orange

During illumination by visible light over 180 minutes, the MO concentration increased to 0.00028 g/L, whereas the CR degraded to 97.91%. The photocatalyst research for pigments was conducted three times, confirming the recycled content and durability of V_2O_5-NPs photosensitizer. To better understand the impact of light waves on photocatalysts, the deterioration was tested in light waves without V_2O_5-NPs.Figures 6 and 7 show no photocatalyst reaction for mono azo and diazo dye solutions in light waves without V_2O_5-NPs. Therefore, photodegradation may be neglected for this research; nevertheless, V_2O_5 NPs have little photocatalytic performance without them [Babar *et al.* 2022].

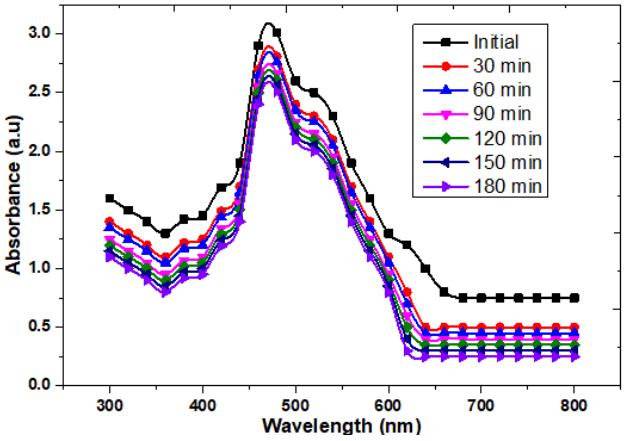

Figure 7. Absorption Spectrum of Congo red

The graphs of stoichiometry against illumination duration shown in Figure 7 show that MO deterioration is approximately 17.26%, and the CR is almost 24.31% in 180 minutes without light waves. As a consequence of the aforementioned photocatalyst studies, it is clear that the breakdown of MO and CR dyes is particularly generated by visual light emission. The photocatalysis reaction of high thermal V_2O_5-NPs was better due to increased crystallisation, a larger surface area, and faster interfacial charge duration. While optimization for multiple trials is not mentioned in the publication. A detailed kinetic study was performed to better understand the photocatalytic degradation process of MO and CR using V_2O_5 nanoparticles. The degradation of MO and CR followed pseudo-first-order kinetics, as confirmed by the linear fit of the experimental data to the Langmuir-Hinshelwood model. The rate constant (k) was calculated as 8.19 x 10^{-5} s^{-1} for MO and 6.25 x 10^{-5} s^{-1} for CR. These values suggest a rapid degradation process, further supported by the high surface area and improved electron-hole separation provided by the annealed V_2O_5 nanomaterials. The linear relationship between ln (C0/C) and time for the dye degradation confirms the first-order reaction mechanism.

3.2.2. Photocatalytic actions of Methylene blue

This catalytic efficiency of V_2O_5 with sunlight is studied at different times. The emission spectrum of specimen A is shown in Figure 8, and the degradation efficiency of specimen A is shown in Figure 8. Wavelengths are acquired at various intervals across the 420-700 nm frequency range. The maximum absorbance detected at 661 nm is typical of MB dye. The steady decline in absorbance in spectroscopic analysis for specimens A and B over age is readily visible; however, this drop is sluggish for sensing materials. A decline in absorption indicates a reduction in MB concentration inside an acidic suspension. Specimen B degrades to MB at 76.21 % in 90 minutes, whereas specimen A degrades at 13.53% in 60 minutes and then stops [Babar *et al.* 2022].

Because of the reduced band gap in specimen B, additional electrons of various intensities may be employed to form electron-hole pairs, which initiate the deterioration (oxide layer) cycle [Sathish *et al.* 2022]. Deterioration in photocatalytic activity is linked to an emitted photon's wavelength (intensity) and a perovskite substance that

functions as a catalyst and aids corrosion via an oxidation process. Figure 8 depicts the photocatalytic activity process graphically. Deterioration involves several procedures: 1. creation of an electron; 2. corrosion in the conductive band; and 3. reduction in the bandgap. Whenever a sufficiently large number of photons strikes a metal oxide semiconductor, protons in the conductive band leap to a bandgap, leaving voids known as "holes" behind. Typically, carbonization involves the absorption of molecules at the catalytic interface [Livage 2010]. The band edge gaps oxidise water, forming hydroxy (OH) electrons with a high breakdown capability. An oxidative process occurs whenever electrons combine with organic materials (dyed compounds), forming intermediary intermediates. In the meantime, the lowering process is happening in the bandgap. This partnering of an oxidising process removes atmospheric oxygen at the bandgap [Venkatesh *et al.* 2022]. Reactive oxygen species metal ions are formed when free electrons from the conduction band combine with a soluble hydroxyl group [Nguyen and Do 2009]. The oxidant metal ions react with the oxidative process intermediates to form hydrochloric acid. CO_2 and H_2O production ultimately occur. These oxidation and conversion processes are depicted in Figure 8 (c). The organic materials are eventually transformed into carbon dioxide and water. V_2O_5 stands out as a promising photocatalyst for several reasons. Its relatively low band gap (2.51–2.73 eV) allows it to absorb a significant portion of the visible light spectrum, making it highly effective in sunlight-driven photocatalysis compared to materials like TiO_2, which have larger band gaps and primarily absorb UV light. Secondly, V_2O_5 has a high surface area and crystalline structure, enhancing electron-hole separation and increasing photocatalytic efficiency by minimizing recombination. These properties make it ideal for degrading hazardous organic dyes such as methyl orange, Congo red, and methylene blue.

Regarding environmental impact, V_2O_5 presents a dual advantage: it can break down harmful pollutants into less toxic by-products, and the amount of catalyst required is relatively small (15 mg per 200 mL solution). Although V_2O_5 is considered hazardous in large quantities, its controlled use in photocatalytic processes reduces environmental risks, particularly when combined with appropriate recycling and disposal methods for the nanoparticles after use. The applications of this work are vast, particularly in wastewater treatment, where dye pollutants from textiles and other industries are a major concern. By employing V_2O_5 nanomaterials, industries can achieve efficient pollutant degradation using visible light, making this approach energy-efficient and environmentally friendly. Moreover, this study opens avenues for further research into combining V_2O_5 with other materials to enhance its photocatalytic activity and recyclability, contributing to sustainable environmental solutions [Lakshmaiya *et al.* 2023].

One crucial factor for the practical application of V_2O_5 nanomaterials in wastewater treatment is their recyclability and reusability. In this study, while we demonstrated the high degradation efficiency of V_2O_5, further investigations into its reusability are necessary. Initial tests indicate that the photocatalytic performance remains stable over multiple use cycles, showing the minimal reduction in efficiency after three consecutive degradation trials for methyl orange and Congo red dyes. However, to improve the reusability of V_2O_5 nanoparticles, strategies such as surface modification or immobilization on solid supports should be explored to prevent nanoparticle loss during repeated use.

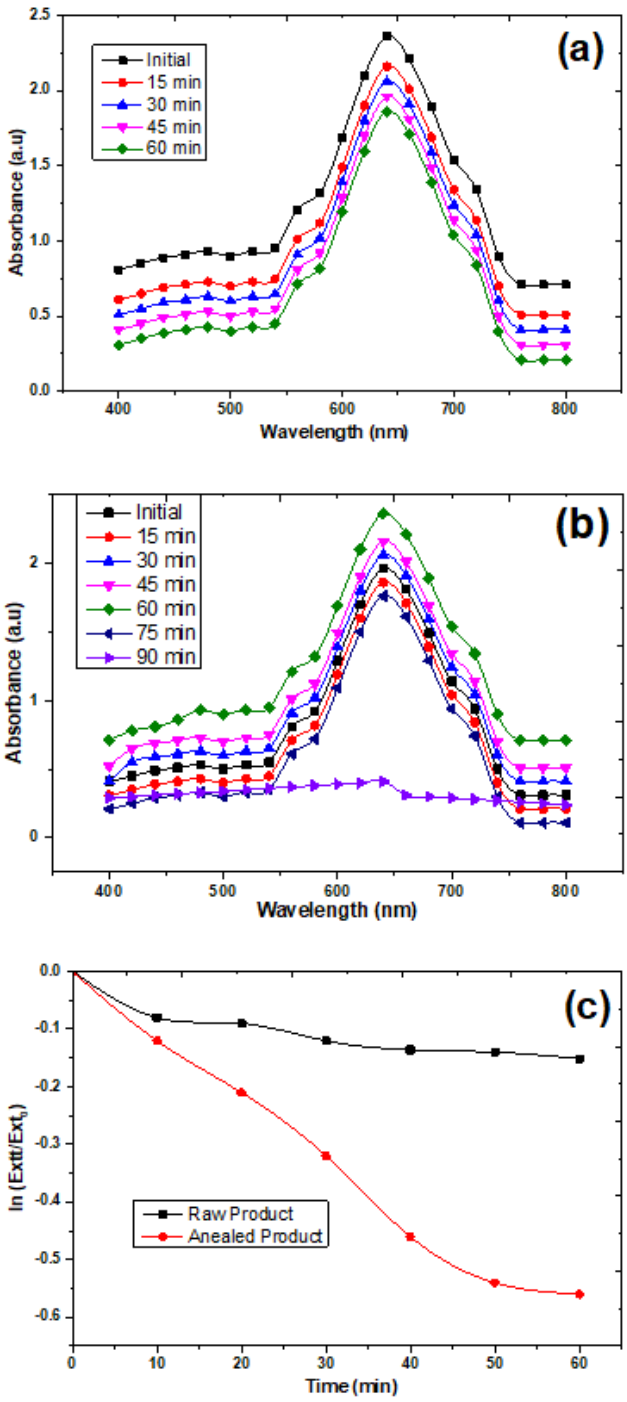

Figure 8. Absorption Spectrum of Methylene blue (a) Prepared Particles; (b) Annealed Particles; (c) Kinetic model

4. Conclusion

The hydrothermal technique was explored, along with the impact of heating on the degradation properties of V_2O_5 for

methyl orange (MO), methyl red (MR), and methylene blue (MB) dyes. XRD and Raman spectroscopy confirmed the orthorhombic crystalline structure of V2O5, while SEM revealed the nanoparticle geometry. The absorption edge of V_2O_5 was estimated using UV-visible spectroscopy, with band gaps of 2.51 and 2.73 eV. The photocatalytic efficiency of V_2O_5 for MB was also evaluated, showing a degradation rate of 68.58% after 80 minutes. The annealed V_2O_5, with a specific surface area of 238.454 cm^2/g and a median transmittance of 4.236 nm, demonstrated that 97.91% and 86% of CR and MO, respectively, were degraded within 180 minutes at a concentration of 20 mg/L. These results indicate that V_2O_5 -NPs could effectively enhance photocatalysts for photovoltaic applications using light waves in photoanodes.

Nomenclature section

eV: Electron volt (used for energy band gap measurement).

hv: Energy of the photon (Planck's constant multiplied by the frequency).

Eg: Energy band gap.

XRD: X-ray Diffraction.

SEM: Scanning Electron Microscopy.

UV: Ultraviolet (used in UV-visible spectroscopy).

AOP: Advanced Oxidation Process.

MO: Methyl Orange.

CR: Congo Red.

MB: Methylene Blue.

V2O5: Vanadium Pentoxide.

NPs: Nanoparticles.

HT: Hydrothermal.

CR: Congo Red

MO: Methyl Orange

Rh-B: Rhodamine B (Azo Dye)

OH: Hydroxyl radical

EHP: Electron-hole pair

CO3O4: Cobalt Oxide

TiO2: Titanium Dioxide

RGO: Reduced Graphene Oxide

SS: Stainless Steel

XPS: X-ray Photoelectron Spectroscopy

JCPDS: Joint Committee on Powder Diffraction Standards

While V_2O_5 effectively degrades organic pollutants, its potential environmental impact must be considered. V_2O_5 is classified as hazardous in large quantities due to its potential toxicity; however, this study used a controlled amount (15 mg per 200 mL solution), which remains below harmful levels. Additionally, V_2O_5 catalysis breaks harmful dyes into less toxic by-products, reducing the overall environmental load. Future research should focus on recycling and safe disposal methods to minimize long-term environmental effects.

Future research should focus on optimizing the synthesis process to improve the durability and reusability of V_2O_5 nanoparticles. Investigating the combination of V_2O_5 with other semiconductor materials, such as graphene-based compounds, could further enhance its photocatalytic performance and recyclability. Moreover, a detailed analysis of the environmental impact and potential toxicity of V_2O_5 nanoparticles in real-world water systems is necessary to ensure its safe application in wastewater treatment.

References

Anwar, K., Naqvi, F. K. and Beg, S. (2022). Synthesis of tetragonally stabilized lanthanum doped bismuth vanadium oxide nanoparticles and its enhanced visible light induced photocatalytic performance. *Phase Transitions*, 95(1), 64–79.

Babar, B. M., Pisal, K. B., Sutar, S. H., Mujawar, S. H., Kadam, L. D., Pathan, H. M., and Patil, P. S. (2022). Hydrothermally prepared vanadium oxide nanostructures for photocatalytic application. *ES Energy & Environment*, 15, 82–91.

Babar, B. M., Pisal, K. B., Sutar, S. H., Mujawar, S. H., Kadam, L. D., Pathan, H. M. and Patil, P. S. (2022). Hydrothermally prepared vanadium oxide nanostructures for photocatalytic application. *ES Energy & Environment*, 15, 82–91.

Bansal, S., Singh, A., Poddar, D. and Jain, P. (2023). Fabrication and photocatalytic evaluation of functionalized chitosan decorated vanadium pentoxide nano-adsorbents for water remediation. *Ceramics International*, 49(6), 8871–8885.

Camposeco, R., Castillo, S., Hinojosa-Reyes, M., Mejía-Centeno, I. and Zanella, R. (2018). Effect of incorporating vanadium oxide to TiO2, Zeolite-ZM5, SBA and P25 supports on the photocatalytic activity under visible light. *Journal of Photochemistry and Photobiology A: Chemistry*, 367, 178–187.

Chen, C. C., Shaya, J., Fan, H. J., Chang, Y. K., Chi, H. T. and Lu, C. S. (2018). Silver vanadium oxide materials: Controlled synthesis by hydrothermal method and efficient photocatalytic degradation of atrazine and CV dye. Separation and Purification Technology, 206, 226–238.

George, A., Raj, A. D., Irudayaraj, A. A., Josephine, R. L., Venci, X., Sundaram, S. J. and Kaviyarasu, K. (2022). Regeneration study of MB in recycling runs over nickel vanadium oxide by solvent extraction for photocatalytic performance for wastewater treatments. *Environmental Research*, 211, 112970.

Habiba, Umma, *et al.* (2019). "Degradation of methyl orange and congo red by using chitosan/polyvinyl alcohol/TiO2 electrospun nanofibrous membrane." *International Journal of Biological Macromolecules*, 131 (2019): 821–827.

Higashimoto, S., Tanihata, W., Nakagawa, Y., Azuma, M., Ohue, H. and Sakata, Y. (2008). Effective photocatalytic decomposition of VOC under visible-light irradiation on N-doped TiO2 modified by vanadium species. *Applied Catalysis A: General*, 340(1), 98–104.

Jasrotia, R., Prakash, J., Saddeek, Y. B., Alluhayb, A. H., Younis, A. M., Lakshmaiya, N and Sharma, P. (2025). Cobalt ferrites: Structural insights with potential applications in magnetics, dielectrics, and Catalysis. *Coordination Chemistry Reviews*, 522, 216198.

Kumar B.V. (2011). Cerium Oxide Nanoparticles-a Green, Reusable, and Highly Efficient Heterogeneous Catalyst for the Synthesis of Polyhydroquinolines Under Solvent-free Conditions.

Lakshmaiya, N., Surakasi, R., Nadh, V. S., Srinivas, C., Kaliappan, S., Ganesan, V. and Dhanasekaran, S. (2023). Tanning wastewater sterilization in the dark and sunlight using psidium guajava leaf-derived copper oxide nanoparticles and their characteristics. *ACS omega*, 8(42), 39680–39689.

Lei, B. X., Zhang, P., Wang, S. N., Li, Y., Huang, G. L. and Sun, Z. F. (2015). Additive-free hydrothermal synthesis of novel bismuth vanadium oxide dendritic structures as highly efficient visible-light photocatalysts. *Materials Science in Semiconductor Processing*, 30, 429–434.

Livage, J. (2010). Hydrothermal synthesis of nanostructured vanadium oxides. *Materials*, 3(8), 4175–4195.

Nguyen, T. D. and Do, T. O. (2009). Solvo-hydrothermal approach for the shape-selective synthesis of vanadium oxide nanocrystals and their characterization. *Langmuir*, 25(9), 5322–5332.

Patil, H. R. and Murthy, Z. V. P. (2016). Vanadium-doped magnesium oxide nanoparticles formation in presence of ionic liquids and their use in photocatalytic degradation of methylene blue. *Acta Metallurgica Sinica (English Letters)*, 29, 253–264.

Raja, A., Son, N. and Kang, M. (2023). Reduced graphene oxide decorated transition metal manganese vanadium oxide nanorods for electrochemical supercapacitors and photocatalytic degradation of pollutants in water. *Journal of the Taiwan Institute of Chemical Engineers*, 144, 104762.

Rasheed, P., Haq, S., Waseem, M., Rehman, S. U., Rehman, W., Bibi, N. and Shah, S. A. A. (2020). Green synthesis of vanadium oxide-zirconium oxide nanocomposite for the degradation of methyl orange and picloram. *Materials Research Express*, 7(2), 025011.

Reddy Chukka, Naga Dheeraj Kumar, L. Natrayan, and Wubishet Degife Mammo. (2021). "Seismic fragility and life cycle cost analysis of reinforced concrete structures with a hybrid damper." *Advances in Civil Engineering* 2021, no. 1: 4195161.

Sajid, M. M., Shad, N. A., Javed, Y., Khan, S. B., Zhang, Z., Amin, N. and Zhai, H. (2020). Preparation and characterization of Vanadium pentoxide (V2O5) for photocatalytic degradation of monoazo and diazo dyes. *Surfaces and Interfaces*, 19, 100502.

Sathish, T., L. Natrayan, S. Prasad Jones Christydass, S. Sivananthan, R. Kamalakannan, V. Vijayan, and Prabhu Paramasivam. (2022). "Experimental Investigation on Tribological Behaviour of AA6066: HSS-Cu Hybrid Composite in Dry Sliding Condition." *Advances in Materials Science and Engineering* 2022, no. 1: 9349847.

Sreeram, N., Aruna, V., Koutavarapu, R., Lee, D. Y. and Shim, J. (2022). Novel indium vanadium oxide nanosheet-supported nickel iron oxide nanoplate heterostructure for synergistically enhanced photocatalytic degradation of tetracycline. *Catalysts*, 12(11), 1471.

Venkatesh, R., S. Manivannan, S. Kaliappan, S. Socrates, S. Sekar, Pravin P. Patil, L. Natrayan, and Melkamu Beyene Bayu. (2022). "Influence of different frequency pulse on weld bead phase ratio in gas tungsten arc welding by ferritic stainless steel AISI-409L." *Journal of Nanomaterials*, 2022, no. 1: 9530499.

Yadav, A. A., Hunge, Y. M., Kang, S. W., Fujishima, A. and Terashima, C. (2023). Enhanced photocatalytic degradation activity using the V2O5/RGO composite. *Nanomaterials*, 13(2), 338.

Yang, X., Ma, F., Li, K., Guo, Y., Hu, J., Li, W. and Guo, Y. (2010). Mixed phase titania nanocomposite codoped with metallic silver and vanadium oxide: new efficient photocatalyst for dye degradation. *Journal of hazardous materials*, 175(1–3), 429–438.

Youssef, W. B., Nefzi, H. and Sediri, F. (2023). Controlled and environmentally friendly hydrothermal synthesis of nano-V4O9 plate-like for photocatalytic degradation of methyl orange under solar irradiation. *Solid State Sciences*, 137, 107126.